

## Impedance and Conductivity Studies of 0.20 Ba (Fe<sub>0.5</sub>Nb<sub>0.5</sub>) O<sub>3</sub>-0.80 SrTiO<sub>3</sub> Nanomaterial

Ritesh Kumar\*, Amarendra Narayan\*\*, N.K.Singh\*\*\*

\*University Department of Physics, V.K.S. University, Ara, Bihar, India

\*\*Dept. of Physics, Patna University, Patna, Bihar, India

\*\*\* University Department of Physics, V.K.S. University, Ara, Bihar, India

Corresponding author : Ritesh Kumar

### ABSTRACT

The impedance and conductivity properties of 0.20Ba(Fe<sub>0.5</sub>Nb<sub>0.5</sub>)O<sub>3</sub>-0.80SrTiO<sub>3</sub> nanomaterial prepared by ball milling induced solid-state reaction technique, in a wide frequency range at different temperatures have been studied. XRD analysis exhibited single phase with cubic structure at room temperature of the present sample. The Nyquist Plot confirmed the presence of both grain and grain boundary effects. The grain and grain boundary resistance decreases with rise in temperature for all the concentration and exhibits a typical Negative Temperature Co-efficient of Resistance (NTCR) transport processes of all The materials. The conductivity spectrum obeys Jonscher's Universal Power Law.

**Keywords**-Impedance, Conductivity, Nyquist Plot, NTCR, Jonscher's Universal Power Law

Date Of Submission: 31-03-2018

Date Of Acceptance 16-04-2018

### I. INTRODUCTION

Barium iron niobate: BaFe<sub>0.5</sub>Nb<sub>0.5</sub>O<sub>3</sub> (BFN) is an interesting high dielectric and environment friendly lead free material. This material evinced high value of dielectric constant ( $\epsilon_r \approx 10^4 - 10^5$ ) covering a wide range of temperature [1-8]. Saha and sinha were first among many researchers who synthesized BFN in 2002.[3-9] Saha and sinha [7] reported that the structure of BFN is cubic whereas Rama et al. [10] indicated that it has monoclinic structure.

Saha and sinha also revealed that BFN is a relaxor ferroelectric material characterized by a broad dielectric transitions with frequency dependent [7]. In order to achieve a better results of BFN powder, a high quality of synthesis should be involved because it is difficult to prepare niobate compounds due to which various approach have been applied to synthesis the BFN powders. Some routes including sol-gel process, hydrothermal and microwave process have been reported for producing the fine BFN powders [11]. However, the costs of starting raw materials for these synthesis routes are quite high. Further, the final product that obtained from these processes is so small. In this article, Ball milling induced mixed oxide synthesis route has been applied to obtain BFN nanomaterial. AC impedance spectroscopy and conductivity studies have performed to get electrical characterization.

### II. EXPERIMENTAL PROCEDURES

0.20Ba(Fe<sub>0.5</sub>Nb<sub>0.5</sub>)O<sub>3</sub>-0.80SrTiO<sub>3</sub> (BFN-ST80) nanomaterial sample was prepared by ball milling induced solid-state reaction technique. High -purity ( $\geq 99.9\%$ ) from M/s Merck specialities private limited ingredients: BaCO<sub>3</sub>, SrCO<sub>3</sub>, TiO<sub>2</sub>, Nb<sub>2</sub>O<sub>5</sub> and

Fe<sub>2</sub>O<sub>3</sub> were used for the preparation. These chemicals were taken in stoichiometric ratio, and mixed in the presence of air for 2 h and in presence of acetone for 6 h. The finely mixed powder was calcined at 1200°C for 8 h. The calcined powder of above mentioned ceramics were regrinded in Ratsche ball milling and used to make pellet of diameter ~10 mm and thickness 1-2 mm using polyvinyl alcohol as binder. The pellets were sintered at 1250°C for 5 h and then brought to room temperature under controlled cooling. The frequency dependence of the impedance and conductivity were measured using an LCR meter in the temperature range from 40°C to 400°C and in the frequency range from 1KHz to 1 MHz.

### III. RESULT AND DISCUSSION

Ritesh Kumar et. al. in their X-Ray Diffraction study of BFN-ST80 sample have reported formation of single-phase with cubic crystal structure.[12 ] They have also investigated its micrographs produced by Field Emission Scanning Electron Microscopy (FESEM) which reveals polycrystalline nature with very compact grain distributions. They have obtain crystallite size of order 20 nm. [12 ]

#### III.1(A) Impedance formalism

Fig.1. shows the variation of  $Z'$  of BFN-ST80 nanomaterial material with frequency at different temperatures (40-400°C). Lowering of barrier layer and release of space charge both of these phenomena can be verified by the observation of convergence of real part of impedance at higher frequencies. Also, the decrease of  $Z'$  with increase in temperature implies a semiconductor like property, and is known

as negative temperature coefficient of resistance (NTCR) behavior.

Fig.2. shows the variation in the imaginary  $Z''$  parts of impedance of the BFN-ST80 nanomaterial material as a function of frequency in temperature range of 40°C to 400°C. As frequency and temperature increase the imaginary part of impedance decreases. Decrease in values of imaginary  $Z''$  with increasing temperature shows an increase in conductivity of the material. The relaxation in BFN-ST80 material is thermally activated which can be analyzed by decrease in  $Z''$  peak as well as its shift towards higher frequency with increase in temperature. All the curves converge at high frequency which implies that in these frequency ranges, a depletion of space charges takes place. [11]

### III.1(B)Nyquist Plot

Fig.3 shows the Cole–Cole plot for BFN-ST80 nanomaterial sample at selected temperature in the range between 40°C and 400°C. ZsimpWin software has been used to analyze electrical circuit model. The values of all parameters are tabulated in Table-1. Implications of the nyquist plots, reveal that ,the straight line graph becomes semi-circular arc with center at real impedance axis with the rise in temperature. This phenomenon is also verified by the decrease in value of  $R_g$  and  $R_{gb}$  with increase in the temperature. This particular property of BFN-ST80 nanomaterial sample shows a semi-conductor like behavior in the sense of a negative temperature coefficient of resistance (NTCR) [13].The variation of grain and grain boundaries conductivity with temperature have been shown in the Fig.4 (a) and (b).The different activation energy related to grain and grain boundaries have been calculated from the Nyquist plot by using Arrhenius's equation.

Also, the presence of Maxwell-Wagner effect is thus confirmed by the large difference between grains and grain boundaries [14]. M-W effect implies involvement of various mechanisms for electrical transport in the grain and grain boundary and an electrically heterogeneous microstructure within the system. The reasonable dielectric responses may be due to the distinctness in activation energy of grain and grain boundary which totally depends on grain and grain boundary micro-structures.

### III.2 Conductive formalism:-

Fig.5 shows frequency – dependent ac conductivity data at different temperatures in the BFN-ST80 nanomaterial sample. At low temperature, conductivity of present sample increases sharply with increase in frequency. This implies the presence of dispersion in conductivity with respect to

frequency. At higher temperatures all the curves for different frequencies show a tendency to merge down, this shows that the dispersion of AC conductivity has narrowed down.

Conductivity of the present sample increases with increase in frequency at higher temperature. Table-2 indicates that the conductivity of the BFN-ST80 nanomaterial sample increases with increase in temperature. As applicable in various materials, Jump relaxation model (JRM) can account for this conductivity behavior with increase in temperature. DC conductivity is independent of frequency which can be attributed to long range movement of charge carriers [15]. Universal dielectric response (UDR) law can be a possible cause in this case of ac conductivity variation with frequency .[16]

The increase in ac conductivity with increasing temperature may be considered as a charge compensation process occurring due to oxygen vacancies created by the loss of oxygen (usually during sintering) which follows Kröger-Vink equation.[17] The activation energy of BFN-ST80 nanomaterial sample has found to 0.27 eV. Long range hopping of oxygen ion between neighboring sites can be a possible cause of this type of relaxation [18].

The temperature dependence of  $\sigma_{ac}(T)$ , at different frequencies for the BFN-ST80 nanomaterial was measured in the temperature range of 40-400 °C. The results obtained are shown in Fig.6 in which  $\ln(\sigma_{ac})$  is plotted as a function of  $(1000/T)$ . It is clear from the Fig. that  $\sigma_{ac}(T)$  for the BFN-ST80 nanomaterial sample shows a frequency and temperature dependence over the whole range of frequencies from 1 KHz to 1 MHz. Fig.7, describes the frequency variation of activation energy for different temperature regions.

Table-3 shows that in High temperature region, the activation energy lies in the range of 2.85 to 0.57 eV, whereas in Low temperature region, the activation energy lies in the range of 0.64 to 0.23 eV. Activation energy for both slopes decreases with increase in frequency, This fall in Activation energies with the increase in frequency exhibits that at lower frequency the long range hopping involves to overcome the high barrier width while the lower activation energy at high frequency involves the short range or localized hopping.Fig.8 and 9 shows the activation energy calculated from linear fit of frequency dependent conductivity ( $\ln\sigma$ ) variation with reciprocal temperature  $(1000/T)$  for BFN-ST80 nanoceramic.

IV. FIGURES AND TABLES

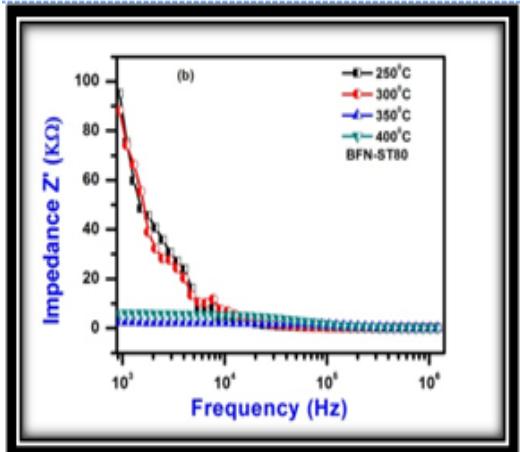
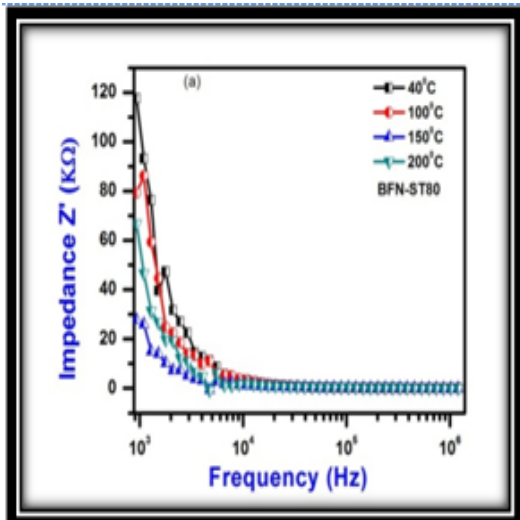


Figure 1. Shows Variation Of Real Part Of Impedance ( $Z'$ ) With Frequency For Different Temperature Ranges In BFN-ST80 Nanoceramic.

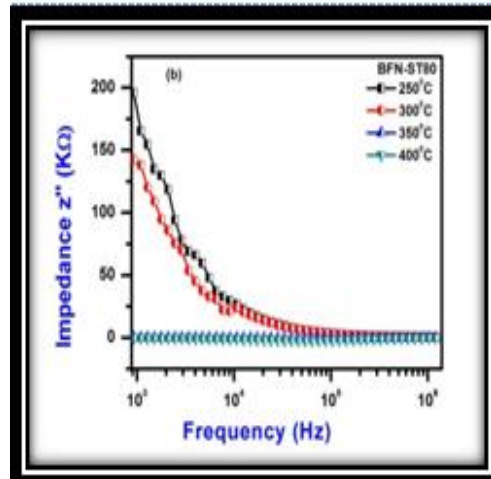
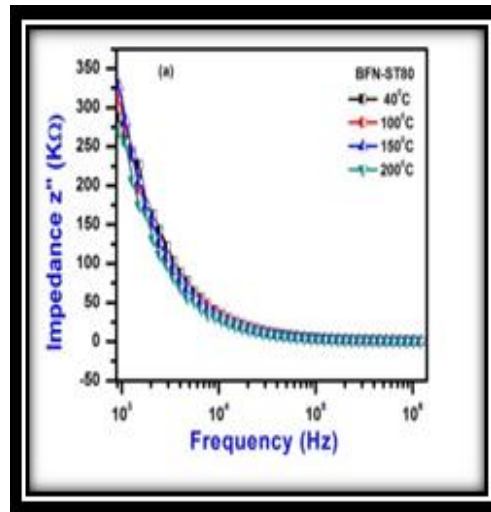
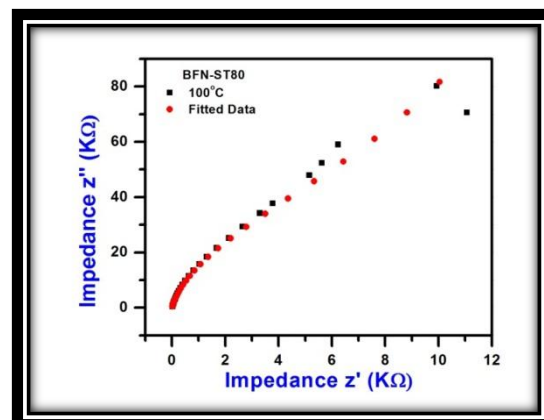
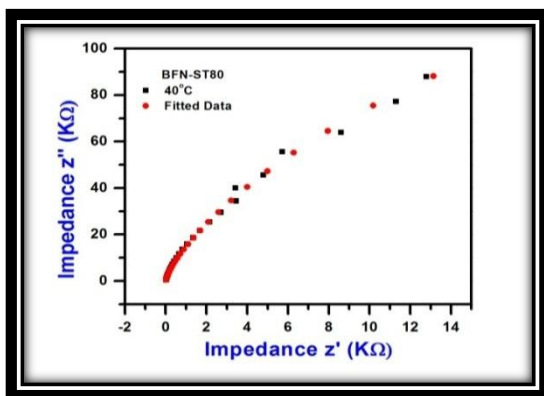


Figure 2. shows variation of imaginary part of impedance ( $Z''$ ) with frequency for different temperature ranges in BFN-ST80 nanomaterial.



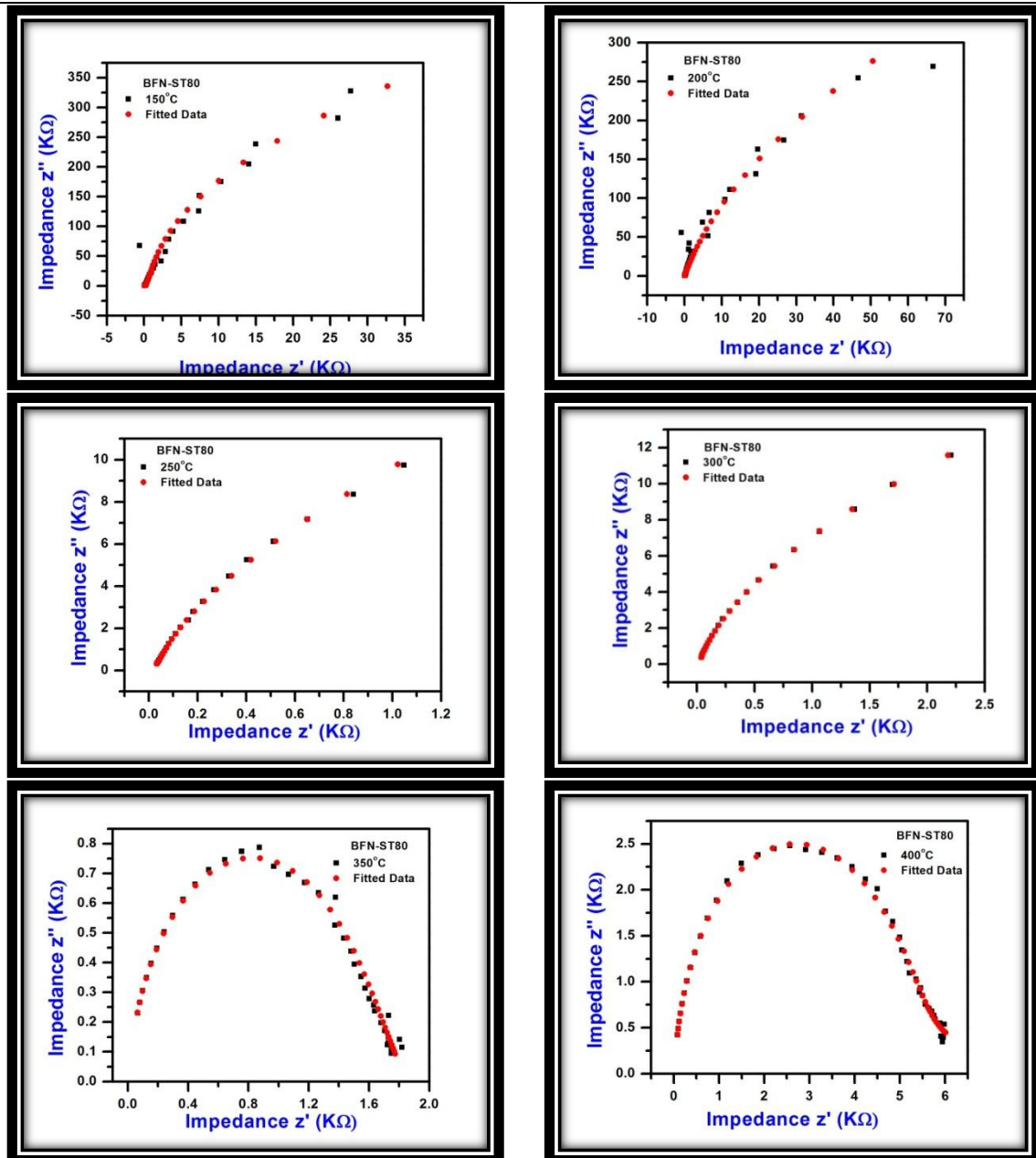
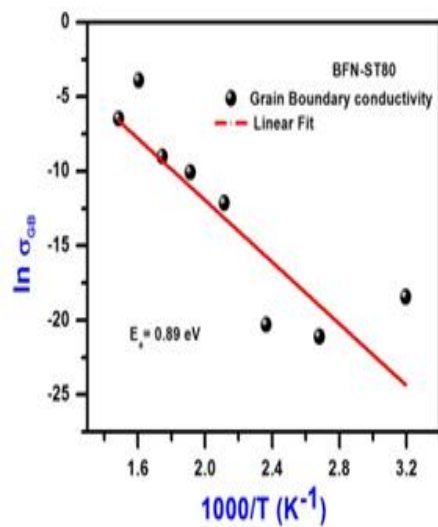
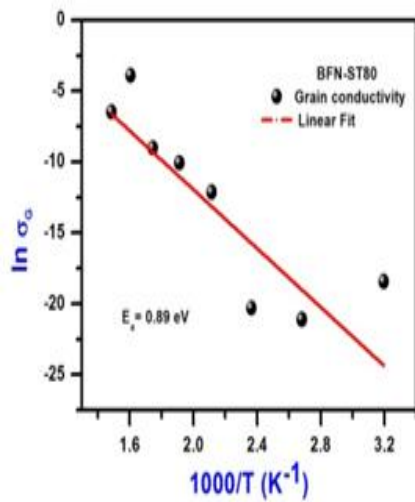
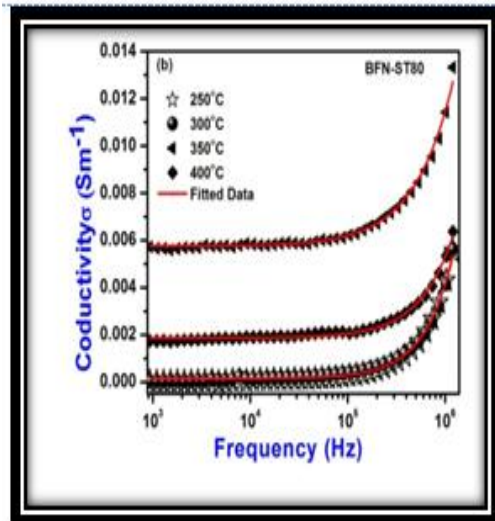
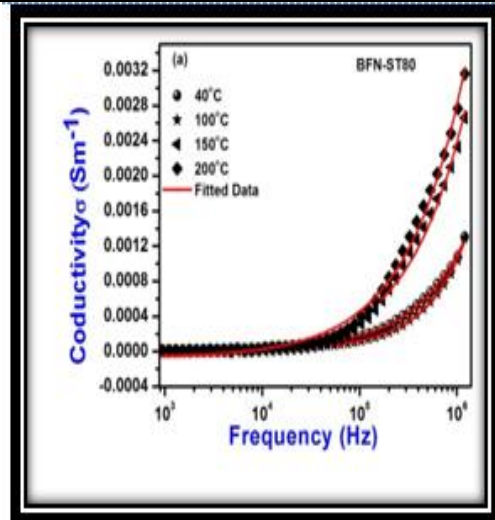


Figure 3. The NyquistPlots Of BFN-ST80 Nanomaterial at different temperature



**Figure 4.** The Arrhenius plots of conductivity ( $\sigma$ ) versus temperature ( $1000/T$ ) for grains and grain boundaries with calculated activation energy of BFN-ST80 nanoceramic sample.



**Figure 5.** shows Frequency dependence behavior of Conductivity at different temperatures.

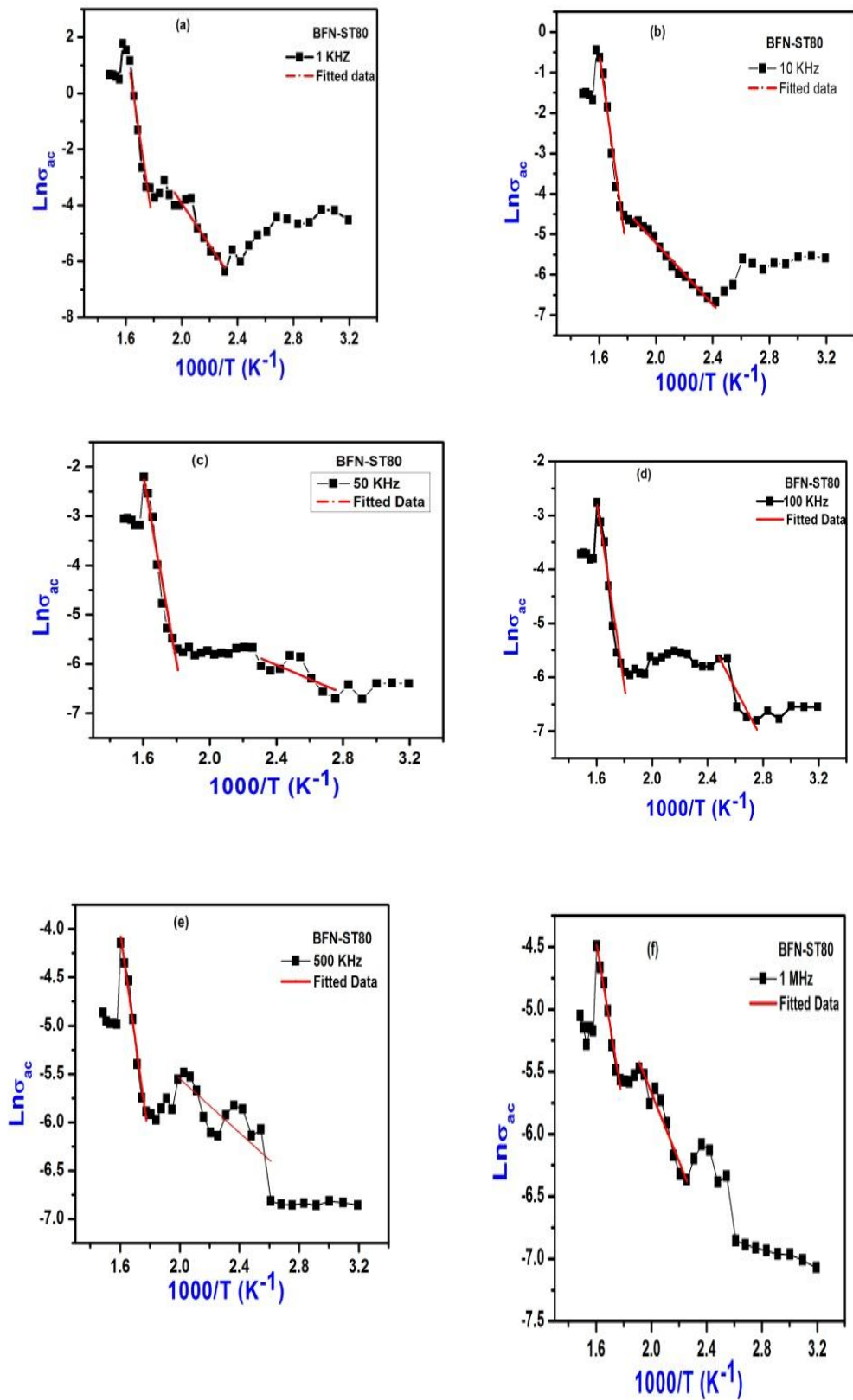


**Figure 6AC** Conductivity  $\text{Ln}(\sigma)$  Variation with reciprocal Temperature ( $1000/T$ ) at different frequencies for BFN-ST80 Nanomaterial

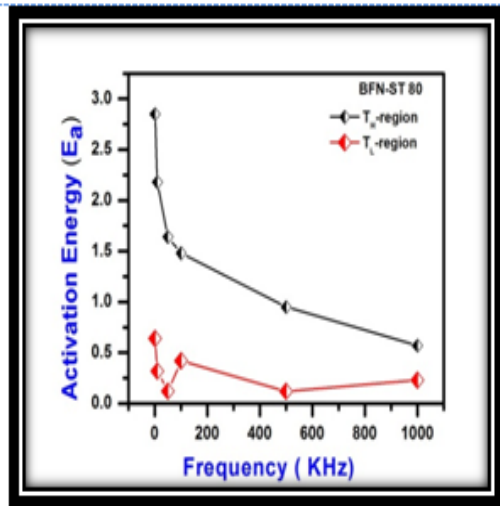


Figure 7. Frequency dependent variation in Activation energy for different conduction regions

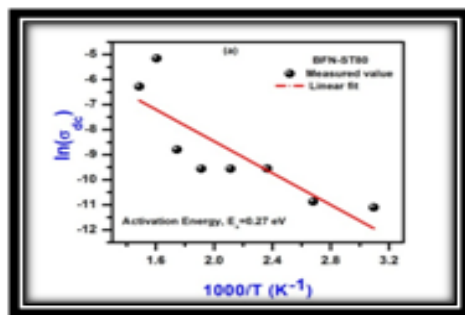


Figure 8 shows the activation energy calculated from linear fit of frequency dependent conductivity ( $\sigma_{ac}$ ) variation with reciprocal temperature ( $1000/T$ ) for BFN-ST80 nanoceramic.

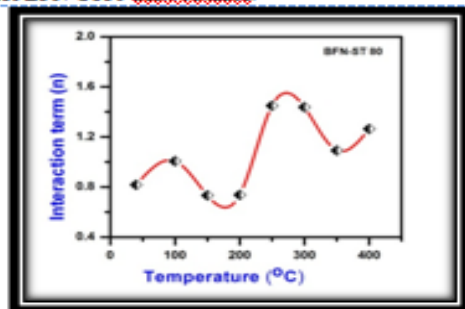


Figure 9 shows the interaction term calculated from linear fit of frequency dependent conductivity ( $\sigma_{ac}$ ) variation with reciprocal temperature ( $1000/T$ ) for BFN-ST80 nanoceramic.

Table 1 .Parameters Of Grain Capacitance ( $C_g$ ), Grain Resistance ( $R_g$ ), Grain Boundary Resistance ( $R_{gb}$ ), And Grain Boundary Capacitance ( $C_{gb}$ ) With

corresponding value of 'n' obtained from the NyquistPlot analysis by considering the electrical equivalent circuits for BFN-ST80 Nanomaterial Sample

Temperature	$C_g$	$R_g$	$C_{gb}$	$R_{gb}$	n
40°C	4.5E-5	7.5E5	1.1E-9	4206	0.7917
100°C	2.5E-9	1.E4	3E-7	8.6E11	0.9766
150°C	5E-10	3.6E6	1.2E-9	9.9E14	0.3426
200°C	2E9	5.6	6.3E-19	2.6E6	0.9516
250°C	4.7E-9	26.6	5.2E-10	3.4E5	0.6301
300°C	1.3E-9	20	4.2E-10	1.1E5	0.773
350°C	1E-9	1139	8.3E-10	709.7	0.5438
400°C	1.9E-9	65.7	4.5E-10	9261	0.1052

Table 2. Different parameters calculated from Universal Dielectric Response (UDR) Law

Temperature (°C)	$\sigma_{dc}$	A	N
40	1.5E-5	1.34E-8	0.81773
100	1.9E-5	9.26E-10	1.00738
150	7E-5	9.7E-8	0.73385
200	7E-5	1.07E-7	0.73802
250	7E-5	8.22E-12	1.44968
300	1.5E-4	9.44E-12	1.43726
350	0.006	1.57E-9	1.09278
400	0.002	8.93E-11	1.26363

Table 3. Activation Energy values for higher temperature and lower temperature relaxation regions for BFN-ST80 Nanomaterial.

Frequency (KHz)	$E_a$ (eV) for High temp. region ( $T_H$ )	$E_a$ (eV) for Low temp. region ( $T_L$ )
1	2.85	0.64
10	2.18	0.32
50	1.64	0.12
100	1.48	0.42
500	0.95	0.12
1000	0.57	0.23

## CONCLUSION

A Ball milling induced solid-state reaction route synthesis was proposed for the preparation of BFN-ST80 nanomaterial. Pure perovskite phase with cubic symmetry was obtained. Impedance study

suggest negative temperature coefficient of resistance (NTCR) behavior of the present sample. Nyquist plot reveal the presence of Maxwell-Wagner effect. Conductivity of the BFN-ST80 nanomaterial sample increases with increase in temperature and follows Jump relaxation model. Since the ball milling induced solid state reaction route shows many advantages for synthesis of lead free electroceramic powder such as BFN-ST, it is interesting to apply it for other lead free materials for future work.

## References

- [1] M.A. Subramanian, D. Li, N. Duan, B.A. Reisner, A.W. Sleight, High dielectric constant in  $\text{ACu}_3\text{Ti}_4\text{O}_{12}$  and  $\text{ACu}_3\text{Ti}_3\text{FeO}_{12}$  phases, *Journal of Solid State Chemistry* 151 (2000) 323–325.
- [2] S. Saha, T.P. Sinha, Low-temperature scaling behavior of  $\text{BaFe}_{0.5}\text{Nb}_{0.5}\text{O}_3$ , *Physical Review B* 65 (2002) 134103–134111.
- [3] C.C. Homes, T. Vogt, S.M. Shapiro, S. Wakimoto, M.A. Subramanian, A.P. Ramirez, Charge transfer in the high dielectric constant materials  $\text{CaCu}_3\text{Ti}_4\text{O}_{12}$  and  $\text{CdCu}_3\text{Ti}_4\text{O}_{12}$ , *Physical Review B* 67 (2003) 092106-1– 092106-4.
- [4] K. Tezuka, K. Henmi, Y. Hinatsu, Magnetic susceptibility and Mossbauer spectra of perovskites  $\text{A}_2\text{-FeNbO}_6$  (A = Sr, Ba), *Journal of Solid State Chemistry* 154 (2000) 591–597.
- [5] M. Yokosuka, Dielectric dispersion of the complex perovskite oxide  $\text{Ba}(\text{Fe}_{1/2}\text{Nb}_{1/2})\text{O}_3$  at low frequencies, *Japanese Journal of Applied Physics* 34 (1995) 5338–5340.
- [6] I.P. Raevski, S.A. Prosandeev, A.S. Bogatin, M.A. Malitskay, L. Jastrabik, High dielectric permittivity in  $\text{AFe}_{1/2}\text{B}_{1/2}\text{O}_3$  nonferroelectric perovskite ceramics (A = Ba, Sr, Ca; B = Nb, Ta, Sb), *Journal of Applied Physics* 93 (2003) 4130–4136.
- [7] S. Saha, T.P. Sinha, Structural and dielectric studies of  $\text{BaFe}_{0.5}\text{Nb}_{0.5}\text{O}_3$ , *Journal of Physics: Condensed Matter* 14 (2002) 249–258.
- [8] S. Eitssayeam, U. Intatha, K. Pengpat, T. Tunkasiri, Preparation and characterization of barium iron niobate ( $\text{BaFe}_{0.5}\text{Nb}_{0.5}\text{O}_3$ ) ceramics, *Current Applied Physics* 6 (2006) 316–318.
- [9] W. Chen, S. Kume, K. Watari, Molten salt synthesis of  $0.94(\text{Na}_{1/2}\text{Bi}_{1/2})\text{TiO}_3\text{-}0.06\text{BaTiO}_3$  powder, *Materials Letters* 59 (2005) 3238–3240.
- [10] N. Rama, J.B. Philipp, M. Opel, K. Chandrasekaran, R. Gross, M.S. Ramachandra Rao, *Journal of Applied Physics* 95 (2004) 7528–7530.
- [11] N. Charoenthai, R. Traiphol, G. Rujijanagul, Microwave synthesis of barium iron niobate and dielectric properties, *Materials Letters* 62 (2008) 4446–4448.
- [12] Ritesh Kumar, Amarendra Narayan, N.K.Singh Structural and Dielectric Characteristics of  $0.20\text{Ba}(\text{Fe}_{0.5}\text{Nb}_{0.5})\text{O}_3\text{-}0.80\text{SrTiO}_3$  nanomaterial, *Int. Journal of Engineering Research and Application* www.ijera.com ISSN : 2248-9622, Vol. 8, Issue 1 , ( Part -IV) January 2018, pp.45-50
- [13] S. Supriya, S. Kumar, M. Kar, *J. Mater. Sci.* 17, 1 (2017)
- [14] Ritesh Kumar, Amarendra Narayan, N.K.Singh, "Structural and Electrical Studies of  $\text{BFN-ST40}$  Nanoceramics Processed By Ball Milling" *International Journal for Research in Applied Science & Engineering Technology (IJRASET)* Volume 5 Issue X, page 2046-2051 (October 2017)
- [15] A. Karmakar, S. Majumdar, S. Giri, *Phys. Rev. B* 79, 094406 (2009)
- [16] A.K. Jonscher, *Universal Relaxation Law* (Chelsea Dielectrics Press, London, 1996)
- [17] F. A. Kröger and H. J. Vink, Relations between the concentrations of imperfections in crystalline solids, *Solid State Phys.* 3, 1956, 307-435.
- [18] A. Dutta, C. Bharti, T.P. Sinha, *Phys. B* 403, 3389–3393 (2008)

Ritesh Kumar "Impedance and Conductivity Studies Of  $0.20\text{Ba}(\text{Fe}_{0.5}\text{Nb}_{0.5})\text{O}_3\text{-}0.80\text{SrTiO}_3$  Nanomaterial" *International Journal of Engineering Research and Applications (IJERA)*, vol. 8, no. 4, 2018, pp. 24-31